Transient current generation during wear of high-density polyethylene by a stainless-steel stylus

J. V. Wasem, P. Upadhyaya, S. C. Langford, and J. T. Dickinson[a)]
Surface Dynamics Laboratory, Department of Physics, Washington State University, Pullman, Washington 99164-2814

(Received 8 July 2002; accepted 5 October 2002)

Contact electrification between metals and insulators lead to dramatic transient charge transfer phenomena during sliding contact. We report simultaneous transient current and lateral force measurements as a stainless-steel stylus is drawn across a high-density polyethylene surface in vacuum. Stylus motion in this system is marked by unstable transitions between high and low velocity modes, similar to stickslip. The high velocity events coincide with falling lateral forces and high current signals. Scanning electron microscope images of the resulting wear tracks show slip-related features at intervals consistent with the lateral force and current fluctuations. Although average charge densities along the wear track ranged from $0.4-1\ \mathrm{mC/m^2}$, measurements at low normal forces are consistent with higher charge densities (up to $3\ \mathrm{mC/m^2}$) at isolated asperity contacts. Current transients as short as 60 μs were observed with total charges consistent with the detachment of $40\times40\ \mu\mathrm{m}^2$ contact areas. © *2003 American Institute of Physics.*
[DOI: 10.1063/1.1525047]

I. INTRODUCTION

Friction and wear of polymers involve the rapid making and breaking of adhesive bonds between asperities, often accompanied by plastic deformation, material transfer, abrasive cutting, and fatigue.[1] We have shown previously that transient currents are often generated when metal–insulator contacts are broken, e.g., during interfacial fracture,[2] peeling,[3–6] or abrasion.[7] These transient currents often reflect the micromechanics of sliding and wear.[8] In previous work, we have described transient currents generated during the abrasion by conducting styli of single-crystal inorganics (including MgO and NaCl),[9] polymers [including poly(methylmethacrylate), polycarbonate, polystyrene, and polyethylene],[7] and metal surfaces in the presence of perfluoropolyether lubricants.[10] A variety of other electrical phenomena, including the emission of charged particles and light, are observed during sliding contact in a vacuum.[11–14] In the case of high-density polyethylene, electron emission during abrasion is many orders of magnitude more intense than emission during fracture of the polymer.[15] This is consistent with the high charge densities that can be left on insulating surfaces when contact with other insulating or conducting surfaces is broken.

This work describes the use of triboelectric currents to probe dynamic processes accompanying sliding contact at a metal–polymer interface. A polyethylene substrate and a conducting metal stylus are instrumented to detect transient electrical currents as the stylus moves across the substrate as well as simultaneous measurements of lateral and normal force. We probe this system over a range of stylus velocities and normal forces where stylus motion is unstable, alternating between high and low velocities in a manner similar to stickslip. This instability yields a rich dynamic behavior that is reflected in both the current and lateral force signals.[6] We show that these currents are a sensitive time-resolved probe of conductor–polymer detachment during sliding.

II. EXPERIMENT

The linear high-density polyethylene (HDPE) employed in this work was commercial material with a density of $0.95\ g/\mathrm{cm}^3$ and a crystallinity of approximately 85%. The material was machined into 3 mm thick sheets and affixed to a translation apparatus with a rapid-curing epoxy. Before each run, the HDPE surface was cleaned with acetone followed by ethanol to remove any contaminants. This treatment was also effective in neutralizing any residual surface charge on the surface. Separate experiments in our laboratory on exchange between liquids such as ethanol and charged polymer surfaces show that the charge readily moves into the liquid and can be carried off by flow.

The experimental apparatus for current, charge, and force measurements is shown in Fig. 1. Abrasion was performed by translating the polymer substrate beneath a stationary conducting stylus (stainless steel) in contact. The conducting stylus was electrically isolated from the support hardware and connected to an electrometer with coaxial cable. The experiment was mounted in a vacuum system (base pressure of 1×10^{-5} Pa) to minimize electrical breakdown. In the presence of a gaseous background, the strong electric fields generated near the stylus–polymer contact due to the charge transfer can ionize the surrounding atmosphere, initiating electrical discharge. Electrical discharges not only produce unwanted electrical transients in our signals, they can reduce the amplitude of the current measured between breakdown events by some orders of magnitude.

The current delivered to the conducting stylus was input directly to the 1 MΩ input of a LeCroy LC334AL 500 MHz

a)Electronic mail: jtd@wse.edu

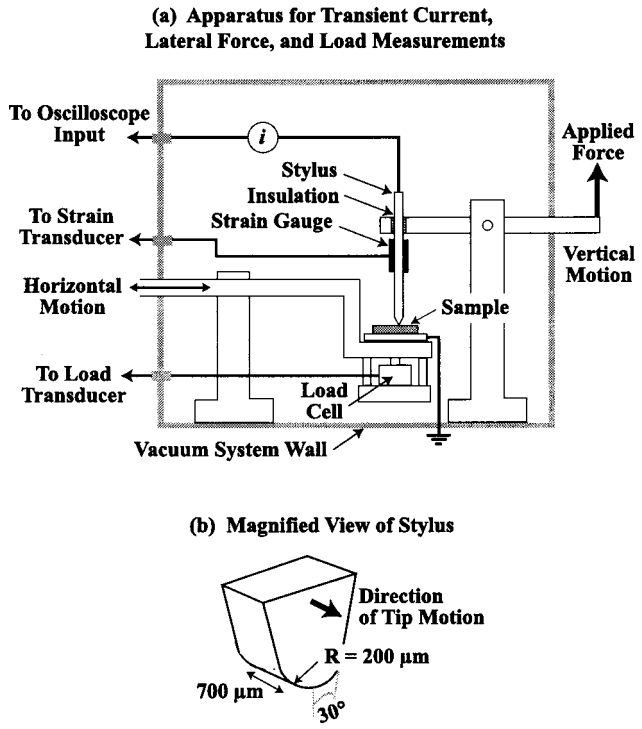

FIG. 1. (a) Schematic of experimental apparatus for lateral force and transient current measurements during tribological loading and (b) approximate stylus dimensions.

digital oscilloscope via a vacuum feed through and coaxial cables (inside and outside). The time constant associated with the input and cable impedances was less than 50 ns. The stylus was machined from a stainless-steel rod 50 mm in length with a rectangular cross section of $1.6\times6\ \mathrm{mm}^2$. The tip of the stylus was machined to a rounded point [see Fig. 1(b)] that was approximated as a cylinder with a radius $R\cong200\ \mu\mathrm{m}$, perpendicular to the direction of motion and thickness $w\cong700\ \mu\mathrm{m}$ parallel to the direction of motion; both the front and rear edges in the thickness direction were rounded with a $\sim50\ \mu\mathrm{m}$ radius to avoid gouging. With this stylus tip, we are clearly in the regime of multiasperity contact. Strain gauges were attached to the stylus and calibrated to indicate the lateral force applied to the tip of the conducting stylus. The strain gauge outputs were fed into an operational amplifier (3 dB cutoff at 1 kHz) and digitized. The frequency response of the amplifier was well above the mechanical resonance of the stylus ($\approx410\ \mathrm{Hz}$), ensuring that the tip motion was accurately sampled. Normal forces were monitored with a Sensotek force transducer mounted beneath the polymer substrate.

Images of the resulting wear tracks were acquired with a JEOL JSM-6400 scanning electron microscope (SEM). Profilometer traces of selected wear tracks were acquired with a SPN Technologies (Goleta, California) PHD Profilometer.

The instantaneous velocity of the stylus tip, $v(t)$, was determined from the lateral force signal, $F_L(t)$, using

$$v(t)=v_0-\frac{1}{k}\frac{dF_L}{dt}, \tag{1}$$

where v_0 is the average velocity imposed on the stylus and $k=3.3\ \mathrm{kN/m}$ is the effective spring constant of the stylus.

III. RESULTS

A. Low average stylus velocity

Contact charging between HDPE and a wide variety of conducting materials (e.g., copper, stainless steel, and tungsten carbide) leaves a positive charge on the conducting material and a negative charge on the HDPE due to electrons donated by the metal to the polymer. This is consistent with the position of polyethylene near the negative end of the triboelectric series.[16,17] Charge is expected to be transferred to the HDPE as electrons and quickly bind to trap sites. Model calculations have shown these traps to be both conformational and bond scission defects with trap energies on the order of 0.2 eV.[18] Although charge transfer occurs during contact, this charge remains close to the interface and does not produce detectable currents until contact is broken. When portions of the contact separate (detach), charge remaining on the conducting phase can then be detected as a current. Sliding contact produces a more or less continuous attachment/detachment cycle, and thus continuous currents are observed.

Typical current and lateral force signals produced at a normal force of 8 N and velocity of 50 mm/s are shown in Figs. 2(a) and 2(b). This normal force corresponds to a nominal stress (normal force/nominal contact area) of about 20 MPa. As expected, sliding of the stylus yields a positive current, indicating that negative charge is transferred from the metal stylus to the polymer. The total detected charge (time integral of current) divided by the nominal area of the wear track was typically $0.4-1\ \mathrm{mC/m}^2$ (negative). These densities were verified by scanning a calibrated charge probe across the wear track immediately after sliding.

Both the current and lateral force signals in Fig. 2 show dramatic fluctuations. Several of the current peaks in Fig. 2(a) are off scale. A plot of instantaneous velocity versus time determined from the lateral force measurements and Eq. (1) is shown in Fig. 2(c). The velocity estimates show a strong oscillation between high and low velocities, with no sign of zero-velocity stick events. The current signal also remains positive throughout the experiment, consistent with the *absence* of zero-velocity stick events; i.e., some detachment is always occurring at all times during sliding.

A small portion of the current and velocity signals are shown on an expanded scale in Fig. 3. The lateral force fluctuations have a sawtooth form, building gradually over several milliseconds and falling sharply, but not to zero, again showing that the stylus moves continuously between the velocity and current maxima. On this time scale, it is clear that the current peaks correspond closely to the velocity peaks, i.e., the current signal is proportional to the instantaneous stylus velocity. No evidence is observed for damped ringing stylus motion after the velocity peaks—the stylus motion is clearly overdamped which is consistent with motion through a highly dissipative medium.

Both the current and velocity signals fluctuate in between the major slip events, although the significance of the

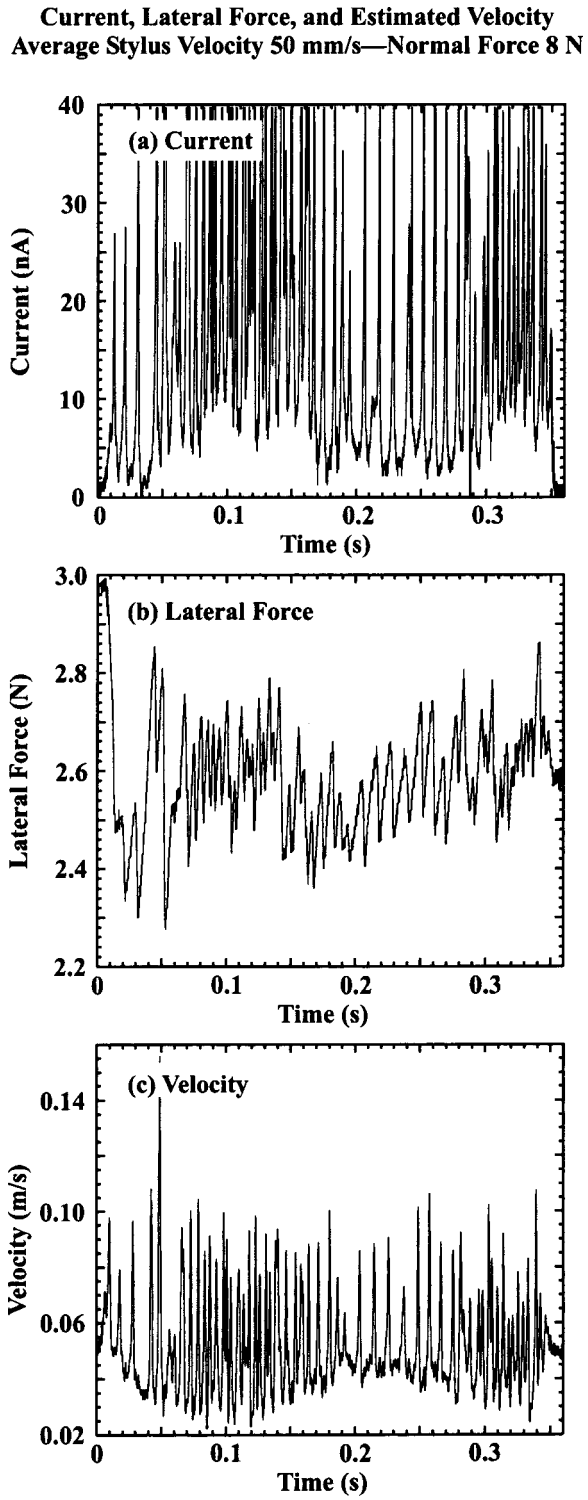

FIG. 2. (a) Current, (b) lateral force, and (c) stylus velocity [computed from Eq. (1)] during the first translation of a stainless-steel stylus over a fresh HDPE surface at an applied normal force of 8 N and average stylus velocity of 50 mm/s. Many of the current fluctuations are off scale.

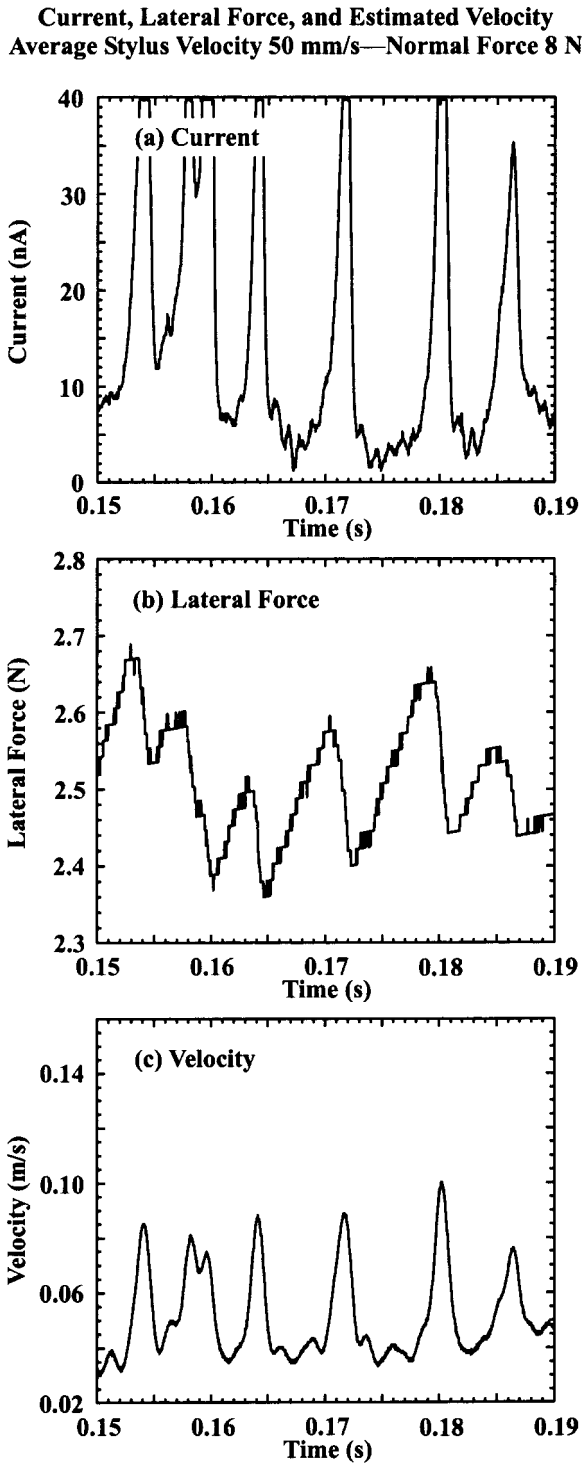

FIG. 3. Expanded view of (a) current, (b) lateral force, and (c) estimated stylus velocity from Fig. 2, showing the close correlation between current and velocity peaks.

smaller velocity fluctuations is clouded by noise in the lateral force signals. The smaller current fluctuations in Fig. 3(a) are well above background noise in the current signal and have a frequency of roughly 1 kHz. Since the resonant frequency of the stylus is only 410 Hz, the entire stylus would have difficulty tracking such rapid motion. We hypothesize that these small fluctuations are due to small detachment events, likely occuring at asperities, that individually have little affect on stylus motion. At a typical charge density of $1\ \mathrm{mC/m^2}$, the sizes of these small fluctuations typically correspond to detached areas of $<500\ \mu\mathrm{m}^2$.

SEM micrographs of the wear tracks also show evidence for plowing in a stick-sliplike fashion. A micrograph of the track for the single pass yielding the signals in Fig. 2 is

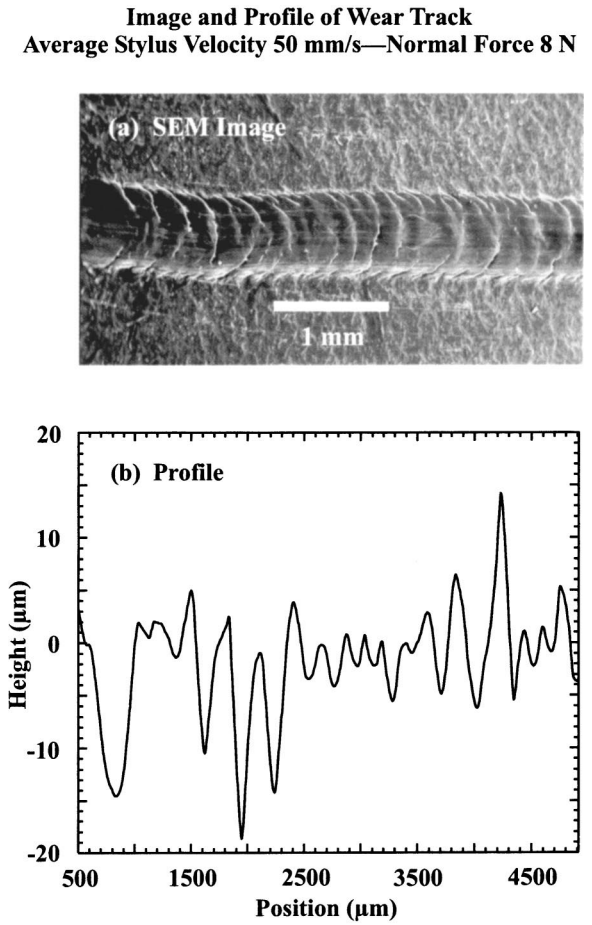

FIG. 4. (a) SEM micrograph of wear track showing quasiperiodic stick slip patterns formed during the wear experiment of Fig. 2. (b) A profilometer trace along the wear track in the general region of the micrograph in (a).

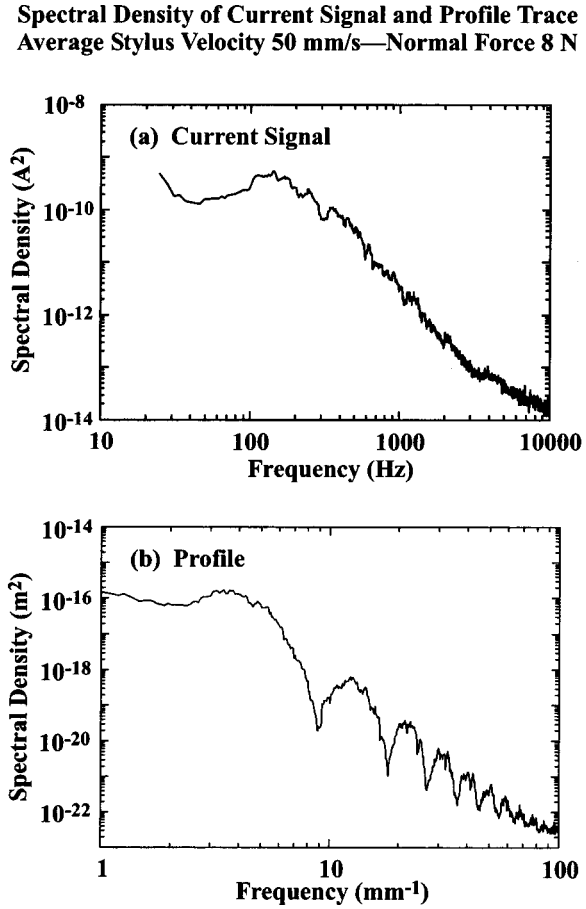

FIG. 5. Power spectra of (a) the current signal of Fig. 2(a) and (b) the corresponding profilometer trace of Fig. 4(b) on log–log scales.

shown in Fig. 4(a). The arclike structures along the length of the wear track correspond to the high velocity portions of the stick-slip cycle, where the depth of the wear track decreases. A profilometer trace of the wear track in this general area appears in Fig. 4(b). The peaks in the profilometer trace correspond to the arcs in the SEM image, and show similar spacings. The average spacing between arcs along the entire wear track, determined from both SEM and profilometry, is about 0.25 mm. The height change associated with the transition from low to high velocity events is highly variable in this profile, ranging from 3 to 20 μm.

Although the fluctuations in current and velocity are not strictly periodic, power spectra of the current and profilometer traces show broad peaks in the low frequencies at roughly 130 Hz and 3.4 mm^{-1}, respectively, as shown in Fig. 5. At an average stylus velocity of 50 mm/s, the average distance between the spatial features (0.3 mm) corresponds to a temporal period of $\sim$6 ms, or a frequency $\sim$170 Hz. This is in reasonable agreement with the frequency of the first peak in the power spectrum of the current signal (130 Hz). The periodic features in the current and profile power spectra can be attributed to the same events, that is, periodic oscillations in the tip velocity.

Both the current and profile power spectra show weaker features at much higher frequencies. The power spectrum of the profile shows a dramatic series of peaks extending out to 100 mm^{-1} (corresponding to features with an average spacing of 10 μm). While the structure of the power spectrum of the current signal is more complex, corresponding features can be identified out to about 2000 Hz. The spacing between the first few peaks is similar to the spacing of normal modes in a cantilever beam fixed at both ends.[19] However, the frequency of the lowest peak (about 130 Hz) is well below the expected resonance of our stylus assuming it vibrates with both ends fixed (about 410 Hz). Thus, we conclude that the low-frequency fluctuations in the current and profile data are due to the viscoelastic response of the polymer substrate.

Both power spectra in Fig. 5 are quite broad, falling with frequency roughly as $1/f^3$, which alone testifies to the rich structure (complexity) of the observed signals.[20,21] The broad low-frequency peaks in both spectra correspond to the frequency/spacing of the major slip events, which occur at a frequency of 100–300 Hz in the current data of Fig. 2 and a spacing of $2-6$ mm^{-1} in the profilometer data (Fig. 4). The power spectrum of the profilometer data, in particular, show a prominent series of peaks that are mirrored weakly in the power spectrum of the current data. The lack of distinct features in the power spectrum of the current is largely due to the fact that the current signal averages the detachment response across the width of the stylus contact area, i.e., the entire width of the wear track. As shown in the SEM image

of Fig. 4(a), many of the slip features extend only partially across the width of the wear track. Because the profilometer samples a single narrow line along the length of the track, local fluctuations are emphasized. Further, one expects the fluctuations along a line to be more correlated than fluctuations on opposite sides of the track. Because the current signal reflects the time average of these fluctuations, high-frequency peaks in the power spectra will tend to be less distinct. We propose that the current signals provide a more faithful representation of this average behavior. By reducing the size (and especially the width) of the stylus, the sensitivity of the current fluctuations to local detachment could be increased.

We attribute the observed velocity instability to the velocity dependence of the viscoelastic response of HDPE. Overlooking the large range of stresses and strains in the polymer near the stylus, it is useful to simply define an average yield stress along the polymer–stylus interface that depends only on stylus velocity. At an average velocity of 50 mm/s and a normal force of 8 N, the stylus produces a wear track about 700 μm wide [Fig. 4(a)]. The stylus itself is 700 μm thick, so that the average stress along the polymer contact (normal force/area) is about 16 MPa. This falls comfortably near the lower end of the typical range of yield stresses (20–40 MPa) reported for HDPE,[22] consistent with the observed plastic deformation during scratching.

B. High average stylus velocity

Typical current and lateral force signals produced at a normal force of 10 N and an average velocity of 110 mm/s are shown in Fig. 6. Note that the average current signal (dq/dt) is higher than at slower stylus speeds [Fig. 2(a)]. At this velocity, the current and lateral force fluctuate continuously. Again, the current peaks correlate well with peaks in the stylus velocity as shown in Fig. 6(c).

Even with an expanded vertical scale, two rapid positive spikes go off scale. Their intensity, sign, and shape are consistent with electrical breakdown. Gaseous breakdown is unlikely in a vacuum. We therefore attribute these current spikes to *surface breakdown*. A more detailed study of these breakdown events has been carried out and a manuscript is in preparation.[23]

A scanning electron micrograph of a portion of the wear track associated with the higher stylus speed data in Fig. 6, along with a corresponding profilometer trace along the wear track, appear in Fig. 7. The micrograph shows a series of arcs appearing at intervals of about 200 μm. This corresponds to the distance between major features in the profilometer trace in Fig. 7(b). The horizontal marks in the micrograph are due to grooves created by asperities on the stylus.

The average normal stress along the stylus/polymer interface during the production of the wear track in Fig. 7(a) was 32 MPa. This is well within the range of yield stresses (20–40 MPa) reported for room temperature HDPE.[22] Since the visible wear track consists of permanently deformed material, we interpret this average stress as a yield stress. At a stylus velocity of 110 mm/s, the range of height fluctuations along the profile (1–7 μm) is considerably smaller than the fluctuations obtained at 50 mm/s [3–20 μm in Fig. 7(b)].

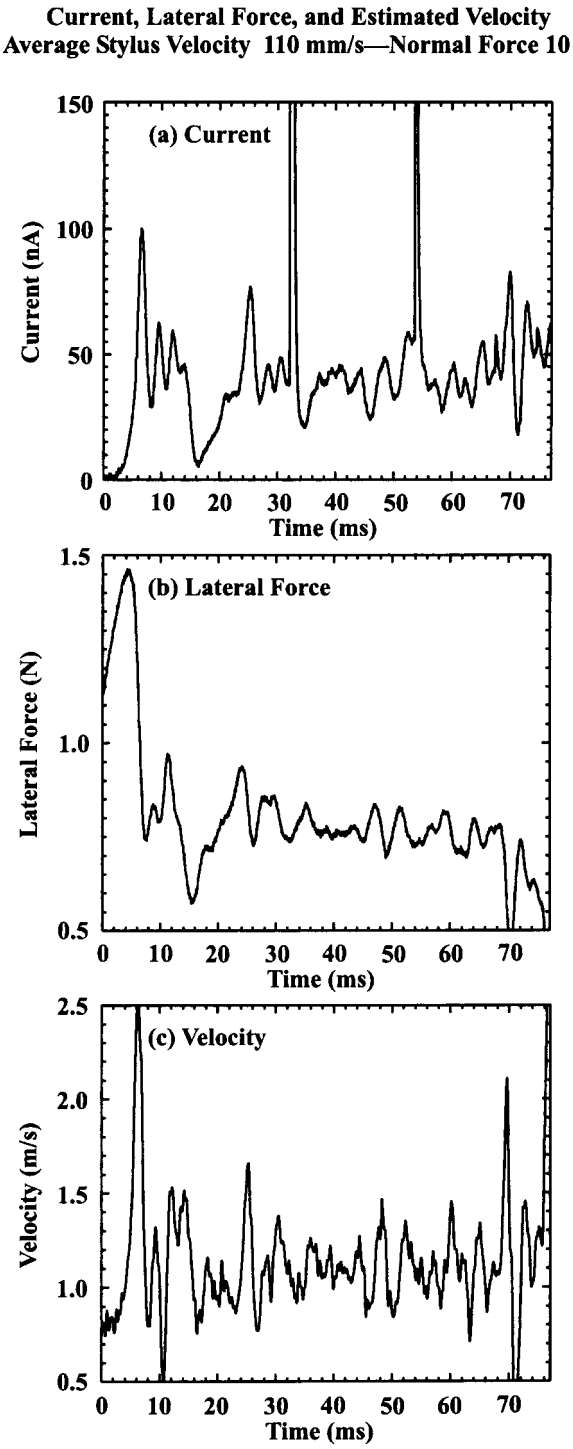

FIG. 6. (a) Current, (b) lateral force, and (c) stylus velocity [computed from Eq. (1)] during the first translation of a stainless-steel stylus over a fresh HDPE surface at an applied normal force of 10 N and average stylus velocity of 110 mm/s. We attribute the two off-scale current fluctuations to electrical breakdown events.

For both stylus velocities, we attribute the observed stick-sliplike behavior to the strain-rate dependence of the yield stress in the polymer substrate. As the stylus velocity (and thus, the yield stress) increases, the contact area required to support the weight of the stylus decreases, allowing

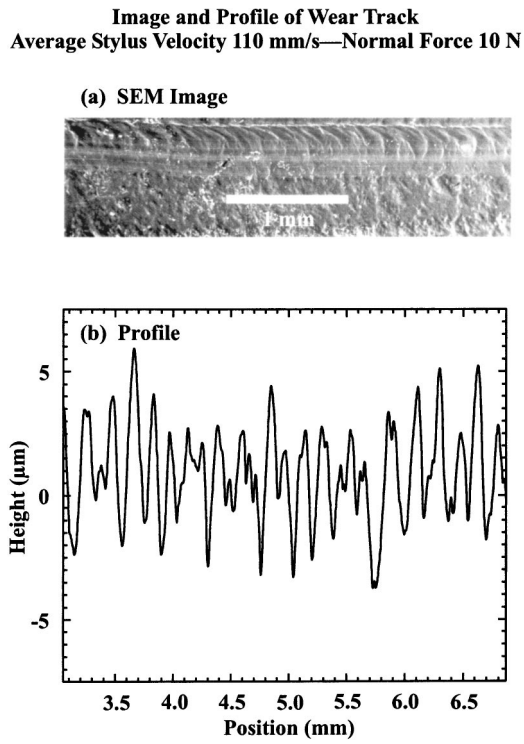

FIG. 7. (a) SEM micrograph of the quasiperiodic stick-slip patterns formed during the wear experiment of Fig. 6. (b) A profilometer trace along the wear track in the general region of the micrograph in (a).

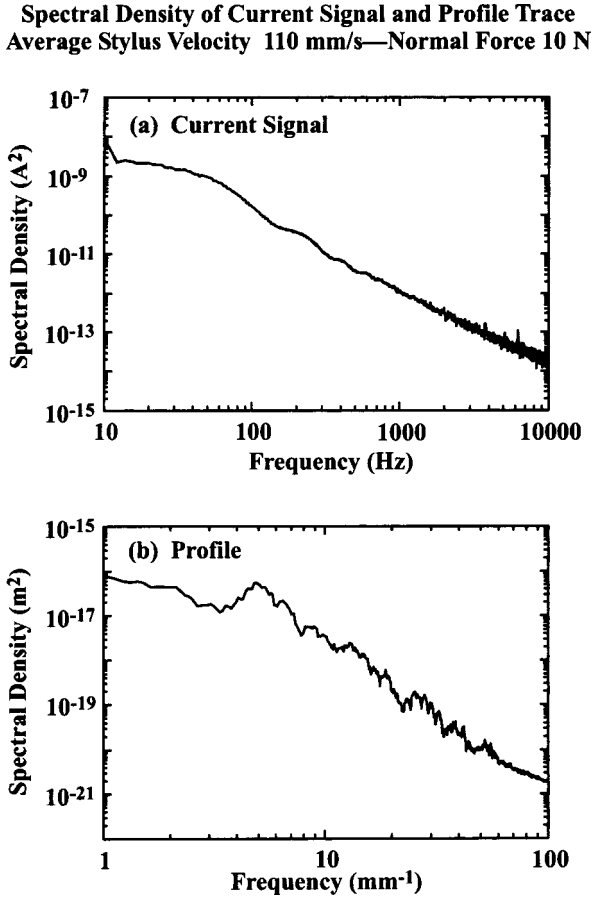

FIG. 8. Power spectra of (a) the current signal of Fig. 6(a) and (b) the corresponding profilometer trace from Fig. 7(b) on log–log scales.

the tip to rise vertically and reducing the depth of the wear track. Because less material is plowed from the wear track at higher velocities, the lateral forces applied to the tip drop as the velocity increases. For instance, the average lateral force on the stylus in Fig. 2 at 110 mm/s and 10 N is about 0.75 N, while the average lateral force in Fig. 6 at 50 mm/s and 8 N is about 2.5 N. Because the lateral force applied to the stylus *decreases* with increasing velocity, the stylus cannot move stably at the imposed velocity.

Power spectra of the current signal in Fig. 6(a) and the corresponding profile trace in Fig. 7(b) appear in Fig. 8. The current and profile spectra show broad low-frequency bands of power at about 500 Hz and 5 mm^{-1}, consistent with the spacings of the major features in the current signal and profilometer trace, respectively. Both sets of fluctuations correlate with the same wear events ($500\,Hz \div 5\,mm^{-1} = 100\,mm/s \approx 110\,mm/s$, the stylus velocity), again confirming the relationship between the velocity fluctuations and the slip-related features observed in SEM images. The current signal shows additional peaks near 2250 and 4000 Hz. Clear peaks in the power spectra of the current signals have been observed at least to 10 kHz. As noted next, faster fluctuations in the current signals (and thus detachment rate) are observed, but the contribution of any periodicity in these fluctuations at higher frequencies in this work is obscured by high-frequency nonperiodic fluctuations.

The power spectrum of the current signal in Fig. 8(a) shows a $1/f^2$ dependence, typical of our current data taken at stylus velocities above 60–70 mm/s. In contrast, the spectrum of the profile data (and current data at lower stylus velocities) falls much more rapidly (about $1/f^3$). Although we do not necessarily expect the current and profile spectra to have the same slope, any mechanical relaxation in the polymer could ''erase'' correlations; in particular, this would have a disproportionate effect on the smaller asperities and reduce the amplitude of high-frequency spatial fluctuations.

Again, these broadband spectra show evidence for rich dynamic structures. In many cases, $1/f^N$ behavior in time series data can be related to complex system dynamics with an effective dimension $D = 5/2 - N/2$.[24] In this case, $1/f^3$ behavior is consistent with $D = 1$ and thus normal, nonfractal dynamics, whereas $1/f^2$ behavior is associated with a nonintegral dimension D, and thus is potentially fractal in character. Nonintegral responses are observed in one-dimensional traces corresponding to Brownian motion,[24] which are associated with chaotic processes. The results of a more detailed analysis of similar fluctuations in current signals generated during peel of a pressure sensitive adhesive were consistent with chaotic character.[6]

C. Rapid detachment events

Many experiments display one or more transient, steplike increases in current that reflect localized detachment events involving failure along the stylus–HDPE interface. The two events in Fig. 9(c) appear on a more compressed time scale in the current signals of Fig. 6(a). On this time scale, the current increases about 12 nA in less than a single

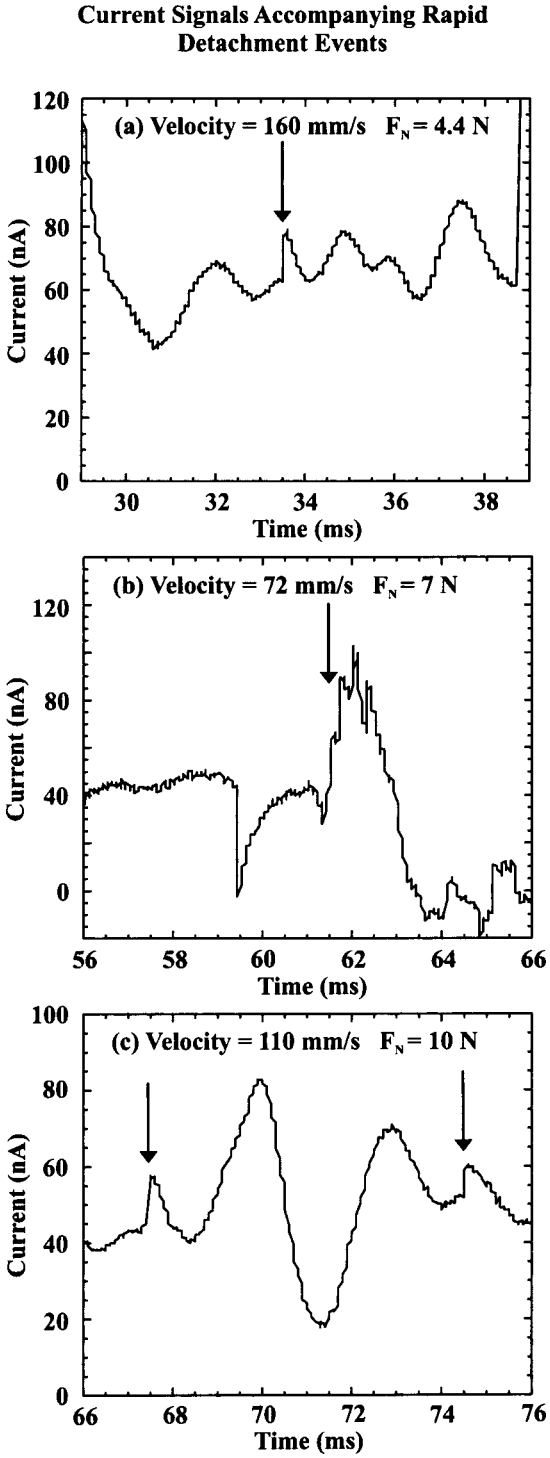

FIG. 9. Steplike increases in current attributed to rapid transient detachment of polymer from the stylus. The transient events in (c) are taken from the current signal in Fig. 6(a).

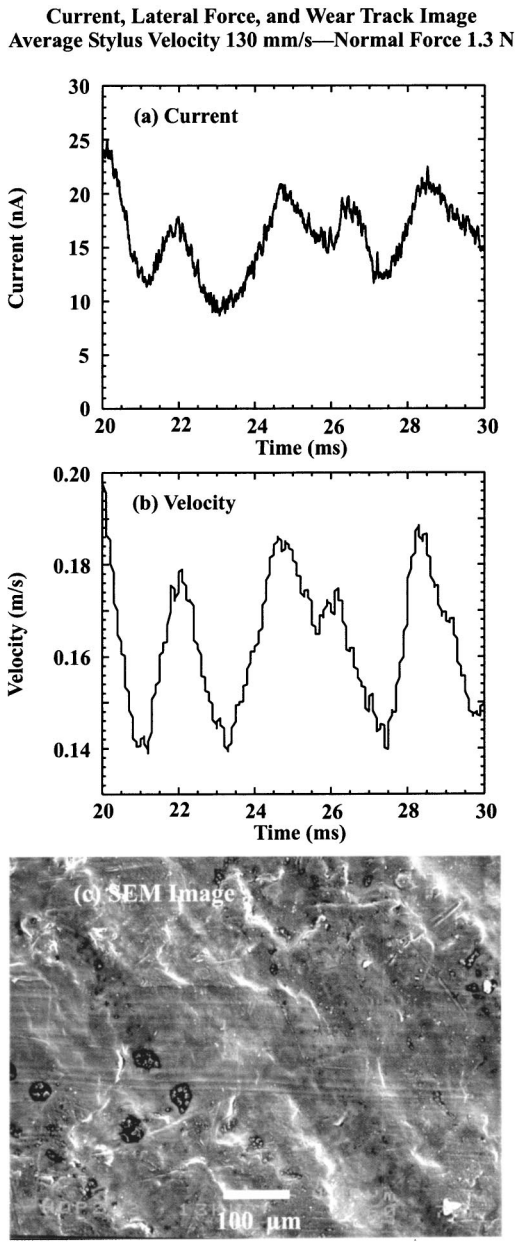

FIG. 10. (a) Current, (b) velocity, and (c) SEM micrographs from a scratch experiment at a contact force of 1.3 N and velocity of 130 mm/s. At this normal force, stylus–polymer contact is principally confined to asperities.

digitization interval (here, 4 μs). Figures 9(a) and 9(b) show similar events during other experiments. Digitized current measurements on faster time scales showed rise times of a few microseconds. These rise times are much slower than rise times associated with electrical breakdown. Conversely, the mass of the stylus is far too great to permit accelerations consistent with these steplike increases. Again, we attribute these jumps to rapid detachment involving small polymer patches, e.g., fingers of material adhering to the stylus. The total charge above the smooth baseline for the event of Fig. 9(a) is about 4 pC, consistent with a detached surface area of about $60\times60\ \mu m^2$. Assuming a square patch, an average detachment or interfacial crack velocity on the order of 0.1 m/s is implied by the 0.5 ms duration of the current peak; the corresponding acceleration at the current step is on the order of $10^5\ m/s^2$ —which is quite feasible for interfacial detachment of a cube of polymer 60 μm on an edge initially attached to the stylus and strained by adhesive forces to stresses somewhat below the yield stress.

D. Current at low contact forces

Figure 10 shows a typical current signal acquired at a low normal force of 1.3 N and average stylus velocity of 130

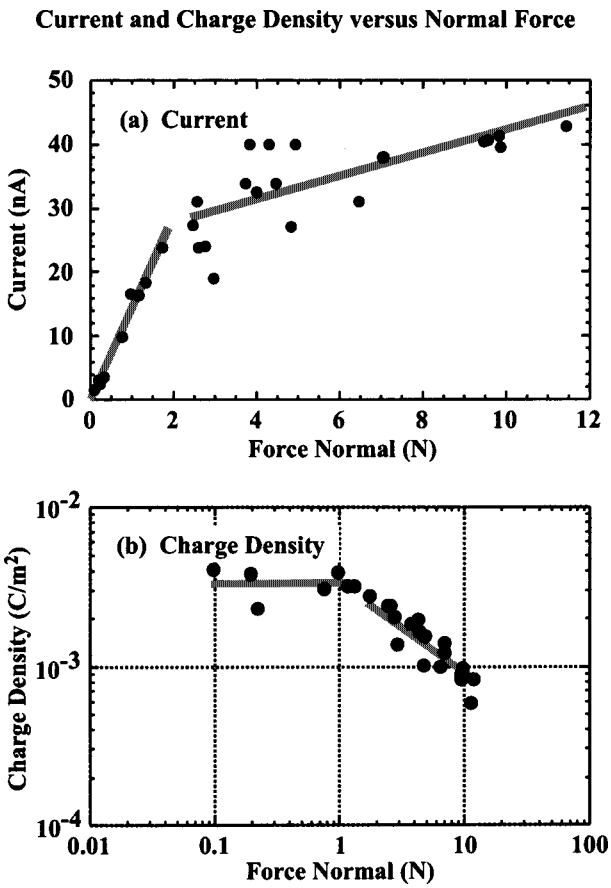

FIG. 11. (a) Average current vs applied normal force, and (b) current density calculated from Eqs. (5) and (6) vs normal force. We identify the break in both curves at about 2 N with the transition from asperity-dominated contact to plowing.

mm/s, along with the instantaneous (relative) velocity determined from Eq. (1) and an SEM image of a small portion of the wear track. At contact forces below about 2 N, a marked change is observed in the nature of the stylus–polymer contact as seen in the SEM images, which show that the passage of the stylus has not significantly altered the polymer surface except at asperities. No signs of arclike structures are observed in the wear track. The correlation between the current and velocity signals is quite good (showing a positive correlation) as seen by comparing Figs. 10(a) and 10(b). Noting that the dimensions of the stylus asperities are quite small relative to the morphological texture of the polymer surface, it is reasonable to suggest that the fluctuations at low normal force are dominated by the surface roughness.

E. Variation in current with normal force

A plot of the average current generated by translation versus the normal force applied to the stylus (F_N) appears in Fig. 11(a). The stylus velocity in these measurements was 110 mm/s. At contact forces below 2 N, the current rises steadily with normal force with a slope of about 14 nA/N. As the normal force increases further, the average currents become more scattered and the rate of current increase (slope) decreases to an average of about 2 nA/N. The onset of erratic average currents corresponds closely to the normal force where arclike structures are first observed in the wear track. We suggest that the mechanical instability responsible for the arcs leads to current fluctuations that yield considerable uncertainties in the average currents. The abrupt change in the slope of the current versus F_N curve is discussed next.

IV. DISCUSSION

A. Origin of currents

No single mechanism of charge transfer between metals and polymers is generally accepted for all metal–polymer systems.[25] The three principal alternatives are (1) bulk material transfer, (2) ion transfer, and (3) electron transfer, where the latter alternatives may involve intrinsic material, defects, and/or impurities.[16]

Material transfer is typically most rapid in the early stages of wear between clean contacts, and rapidly decreases in importance.[26] A small amount of HDPE is transferred to the stylus in our work, and failure to remove this transferred material after each experiment does alter the observed current. Nevertheless, if charge transfer were primarily due to transferred material, we would expect high currents at the onset of a single scratch and lower currents thereafter. (Most material is transferred near the beginning of the wear track.) This behavior is not observed in our work, and is not observed in contact charging experiments with similar metal–polymer systems.[26] Thus, we rule out material transfer as the source of the observed currents.

Ion transfer has been implicated in polymer systems with reactive groups (e.g., OH^-) that can release protons. For instance, proton transfer has been implicated in the contact charging of octadecanol-doped HDPE.[27] Although the hydrogen bonds along the HDPE backbone are believed to be stable with regard to proton transfer, there is concern that impurities, perhaps oxidation products, may serve as proton donors or electron acceptors. The possible role of oxides is discussed below.

Several measurements of charge transfer between metals and polymers (including HDPE) in a vacuum have shown correlations between the sign and amount of charge transfer and the metal work function. The relations are not always simple, but they strongly implicate the electron as the mobile charge.[28–30] Contact charging of HDPE by steel in vacuum has recently been shown to increase subsequent photoelectron emission intensities at low photon energies (<3 eV) by some orders of magnitude,[31] also consistent with electron transfer from the stylus to the polymer. The fact that the metal (essentially grounded through the oscilloscope) is an infinite supply of electrons explains why we can continue to generate current by reciprocal motion of the stylus; the other charge transfer mechanisms would tend to be finite.

Electron transfer to the polymer requires suitable electron states. The nature of these states has been debated extensively. The primary candidates include conformational defects (e.g., strained carbon–carbon bonds associated with gauche defects), broken-chain induced defects, and impurities.[18]

Several lines of evidence, including electron microscopy, indicate that the transferred charge is distributed in the near-

surface bulk. Measurements of this depth range from a few nm[32] to several microns,[33–35] suggesting that most of the transferred charge ends up in bulk states, as opposed to surface states. Further, the dispersion of transferred charge accelerates dramatically at temperatures where various molecular motions along the HDPE backbone become active.[36] Thus, it is likely that intrinsic backbone structures, or combinations of these structures, serve to trap charge. The associated energy levels are strong functions of local molecular environment, allowing for a significant range of trap energies. Further, states participating in initial charge transfer may not be the same as those responsible for long-term trapping. Transferred electrons would gradually accumulate in the lowest lying traps, which may be distributed well into the bulk.

Oxidation products can dramatically enhance charge transfer between HDPE and various metals.[37,38] To test for possible oxide involvement, we performed a series of experiments on fresh HDPE surfaces formed by smoothly gouging the material in air and promptly mounting it in vacuum. The scratched material yields significantly higher currents than as-received (and thus oxidized) HDPE. This is consistent with observations of enhanced contact charging on damaged HDPE. For instance, electron emission induced by metal–polymer detachment in a vacuum is much more intense from damaged HDPE than from undamaged HDPE.[15] Similarly, damaged polytetrafluoroethylene (PTFE) yields higher charge densities in contact charging measurements than undamaged PTFE, which is attributed to the generation of electron traps by bond breaking.[39] Through long exposure to the atmosphere, the material employed in our work is oxidized. We suggest that electron acceptor states generated during wear track formation are more important in current generation than the oxide states responsible for charge transfer in significantly more gentle contact charging experiments.

B. Origin of stick slip

Both the current and lateral force data indicate that the stylus velocity remains well above zero, despite the presence of a stick-sliplike velocity instability. In contrast, the velocity instability in the archetypical stick-slip system is driven by the difference between the kinetic and static coefficients of friction and involves true, zero-velocity stick events between slip events. Zero-velocity stick events have been observed during the scratching of a styrene–acrylonitrile copolymer, for intance.[40] The origin of the velocity instability in our experiment thus deserves further explanation.

As noted herein, we attribute the velocity instability in this work to the strain-hardening behavior of HDPE. The yield stress, σ_y, is a logarithmic function of strain rate over a wide range of strain rates for many polymers,[41] including HDPE.[42] Although the complex polymer flow at the stylus–polymer contact would be difficult to model completely, it is reasonable to assume that the strain rate in some nearby region controls the overall behavior of the contact, and that this strain rate is proportional to the stylus velocity. That is,

$$\sigma_y = \sigma_0 + \alpha \ln(v/v_0) = \alpha \ln(v/v^*), \tag{2}$$

where σ_0 is the effective yield stress at velocity v_0, α is a constant, and v^* is a scale velocity chosen to ensure equality. The wear track widths and corresponding yield stress estimates from Figs. 4(a) and 7(a) are consistent with $\alpha \sim 20\,\mathrm{MPa}$ and $v^* \sim 23\,\mathrm{mm/s}$. Equation (2) is valid only when v is significantly greater than v^*, to avoid the unphysical prediction of zero (or negative) yield stress.

The nature of the velocity instability is described by a simple rigid-plastic model of polymer–stylus contact, where the polymer is rigid at applied stresses below the yield stress and displays ideal plastic behavior when the yield stress is exceeded. A similar model successfully accounted for the variation in lateral force with normal force and velocity during wear track formation in a soft particle composite.[43] In this case, the entire normal force, F_N, must be supported by a surface area (component parallel to the plane of the surface), A_N, so that

$$F_N = \sigma_y A_N. \tag{3}$$

Similarly, we estimate the lateral force exerted by the polymer on the stylus (plowing force) by the product of σ_y and the area of the stylus–polymer interface perpendicular to the surface, A_L:

$$F_L = \sigma_y A_L. \tag{4}$$

The relationship between A_N and A_L is determined by the stylus geometry. For small area contacts, our stylus geometry is approximately described as the cross section of a cylinder with radius $R \approx 0.27\,\mathrm{mm}$ perpendicular to the direction of motion and thickness $w \approx 0.7\,\mathrm{mm}$ parallel to the direction of motion as shown in Fig. 1(b). Assuming that A_N is sufficient to support the stylus, the corresponding A_L is

$$A_L = \frac{R^2}{2}\left\{2\arcsin\left(\frac{F_N}{2Rw\sigma_y}\right) - \sin\left[2\arcsin\left(\frac{F_N}{2Rw\sigma_y}\right)\right]\right\} \approx \frac{F_N^3}{12Rw^3\sigma_y^3}, \tag{5}$$

where the later relation applies in the limit of small contact areas. Although this limit is not strictly met, the simplification does not significantly affect our conclusions.

The resulting equations of motion are highly nonlinear, but the necessary physical insight is obtained by examining a simplified form neglecting inertial effects. Equating the lateral force applied by the stylus [See Eq. (1)] to the viscous or yield force applied by the polymer gives:

$$\frac{F_N^3}{12Rw^3\sigma_y^2} = -k(x - v_0 t). \tag{6}$$

Simplifying and substituting the expression for σ_y from Eq. (6) yields

$$\frac{\gamma}{\ln^2(v_0/v^*)} = -k(x - v_0 t), \tag{7}$$

where $\gamma = F_N^3/(12\alpha^2 Rw^3)$. Further simplification is obtained if we consider only deviations of the stylus from the "zero-force" position, $x = v_0 t/k$. Setting $y = (x - v_0 t)$, yields

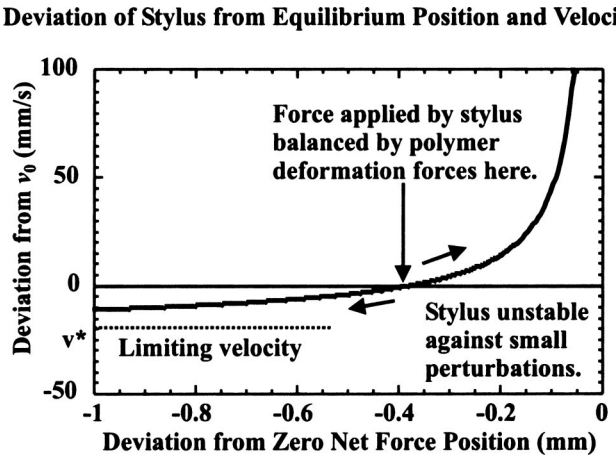

FIG. 12. Diagram of stylus trajectory, showing how the instantaneous stylus tip velocity dy/dt (measured relative to the imposed velocity v_0) is expected to vary with tip position y (measured relative to $v_0 \times t$). The stylus is unstable with respect to small deviations from the equilibrium position. The low velocity branch of this curve displays an asymptote at $v^* \approx 23$ mm/s.

$$\frac{\gamma}{\ln^2\left(\dfrac{dy/dt + v_0}{v^*}\right)} = -k\,y, \tag{8}$$

which has physical solutions only for $y<0$ and which satisfy

$$\frac{dy}{dt} = -v_0 + v^* \exp\left[\left(\frac{-\gamma}{k\,y}\right)^{1/2}\right]. \tag{9}$$

A plot of dy/dt versus y is shown in Fig. 12. If the slope of this plot is negative where it crosses the $y=0$ axis (where the stylus moves at the imposed velocity), the corresponding velocity (dy/dt) will drive the stylus back toward the equilibrium position at $y=0$. The positive slope of the dy/dt versus y plot implies that small perturbations about the equilibrium point $y = -\gamma/[k \ln^2(v_0/v^*)]$ will grow rapidly. Having neglected inertial effects and practical limits on strain hardening, perturbations in the $+y$ direction grow without bound. This corresponds to the high velocity portion of the stick-sliplike instability. At some point, the stylus trajectory must leave the plotted curve and return to the slow velocity branch as dy/dt drops to negative values. Similar perturbations in the $-y$ direction grow and approach the limiting velocity v^* from above. In practice, the low velocity perturbations are limited by the failure of the constitutive equation. As the stylus velocity drops, the yield stress does not continue to drop but plateaus. Prior to this point, the lateral force applied by the stylus must exceed the lateral force required to plow through the polymer, forcing the stylus trajectory off the low velocity branch to the high velocity branch as dy/dt rises to positive values. No physical solution incorporates points corresponding to $dy/dt = -v_0$ ($dx/dt = 0$). Thus zero-velocity stick is not expected within the limits of this model.

The model predicts a minimum stylus velocity of v^* ($dy/dt = -v_0 + v^*$). Data taken at the lower end of the experimental velocity range [Figs. 2(c) and 3(c)] show minimum velocities of 25–40 mm/s, comparable to the predicted minimum of $v^* \approx 23$ mm/s. Further, this minimum is often sustained for several hundred microseconds; in the context of the model, stylus motion has stayed on a low velocity branch long enough to approach v^*. At higher imposed velocities, as in Fig. 6, the velocity and current signals show no evidence of a plateau between spikes and the minimum velocities are somewhat higher. At these imposed velocities, the stylus does not remain on the low velocity branch of the trajectory long enough to approach the minimum.

We note that experimental observations of the predicted velocity instability require a sufficiently compliant stylus. Raising the stylus spring constant in this work by a few orders of magnitude, for instance, would ensure that displacements from the equilibrium point $y = -\gamma/[k \ln^2(v_0/v^*)]$ remain small and generally undetectable. This accounts for the absence of an instability in Briscoe's measurements during wear of a solid particle composite.[43]

C. Effect of instantaneous velocity and normal force on current

The rigid-plastic model of polymer contact can be extended to describe how the observed current depends on instantaneous velocity and normal force. At high contact forces, where the stylus makes more or less uniform contact with the polymer, the contact area is simply related to the geometry of the stylus. The magnitude of the observed current, I, is then proportional to the product of the area detached per unit time and instantaneous charge density σ_q on the detached polymer:

$$I = L\,v\,\sigma_q, \tag{10}$$

where L is the length of the contact zone where metal–polymer detachment occurs. With the aforementioned tip geometry and ignoring asperities,

$$L = 2R \arcsin\left(\frac{F_N}{2Rw\sigma_y}\right). \tag{11}$$

Throughout the experimental range of normal forces, $\arcsin(\theta) \sim \theta$ so that the current is a linear function of the normal force and independent of stylus curvature:

$$I \approx \frac{v\,\sigma_q F_N}{w\,\sigma_y}. \tag{12}$$

This relation also applies in the limit of asperity contacts, as long as the asperities are of fixed length w, parallel to the direction of motion. Other geometries for asperity contact are not supported by the data, which show a linear relation between current and F_N at low normal forces.

The initial slope of the current versus normal force plot in Fig. 11(a) provides an independent estimate of the local charge density. With $v \approx 110$ mm/s, $w \approx 0.7$ mm, and $\sigma_y \approx 32$ MPa, the initial slope of 14 nA/N corresponds to a deposited charge density of about 2.8 mC/m^2, while at higher normal forces, the observed slope of 2 nA/N yields a surface charge density of about 0.4 mC/m^2. Charge density estimates

using measured wear track widths at normal forces above a few N (where the wear track contact area can be reasonably estimated) range from 0.4 to 1 mC/m^2.

Due to the difficulty of accounting for the contribution of asperity contact to the total contact area, it is convenient to estimate this area from F_N and the yield stress given by Eq. (2). Solving Eq. (12) for the surface charge density then yields

$$\sigma_q = \frac{Iw\alpha \ln(v/v^*)}{vF_N}. \tag{13}$$

A log–log plot of the resulting charge density versus F_N is shown in Fig. 11(b). Again, a transition appears at normal forces of 1–2 N, where we observe a transition between asperity dominated contact and smooth contact along the middle of the wear track.

We attribute the drop in charge density at high normal forces to charge recombination made possible by the formation of a continuous patch of abraded material along the length and width of the wear track. As the stylus moves along the polymer surface, the charge left along the wear track is reduced by charge flow *back* to the stylus. In asperity dominated contact, the lack of a smooth, horizontal path from recently exposed polymer to the stylus can reduce these currents, due to the low carrier densities in the trenches between asperities. In addition, uncharged material between asperities will reduced the average electric field along the wear track and thus reduce the driving force for recombination. The importance of recombination at higher normal forces is indicated by the presence of occasional breakdown events. These events reflect extremely large, but short lived, recombination currents, which are the subject of an ongoing study.[23]

D. Potential sensitivity of current measurements to detachment events

Isolated current transients as short as 60 μs have been observed in this work. The power spectra of the current signals show evidence for small fluctuations with similar durations. Standard electronics can easily detect transient currents of 10 nA over time scales of 100 ns. At the charge densities observed in this work, such a current would be produced during detachment along a 1×1 μm^2 patch of interface at interfacial crack velocities on the order of 10 m/s. This rise time for the detection of such signals is limited primarily by the input capacitance and resistance of the measuring device. From circuit analysis, the decay time of transient signals can be significant if the sample capacitance is not kept small. In the aforementioned geometry, the decay time toward the end of a wear track, where the capacitance is highest, approaches 1 μs. Therefore, both the rise and fall of transient signals can be accurately followed up to frequencies of 1 MHz. Improvements in sample geometry (increased sample thickness, shorter wear track) and sensitivity could improve this significantly. We are currently extending these measurements to probe transient asperity contact in insulator/metal systems on submicrosecond time scales.

V. CONCLUSIONS

The transient current signals generated during sliding contact between a stainless-steel stylus and a polymer substrate are strongly affected by local fluctuations in the rate of detachment. In this work, the principal fluctuations are driven by an instability in the stylus–polymer contact. A simple rigid-plastic model incorporating the dependence of yield stress on velocity accounts for the instability and the presence of a lower bound on the velocity that prevents true stick: Neither the velocity nor the current drops to zero. The magnitude and frequency of these fluctuations is limited by the frequency response of the stylus, which here amounts to a few hundred Hz.

The high amplitude and time resolution of the current measurements has easily resolved detachment events involving 40×40 μm^2 patches of polymer over submillisecond time scales. The sensitivity of the instrumentation suggests that much smaller (<1 μm^2) and faster (>1 MHz) detachment events could be detected. Such small/rapid detachment events would not be detected in conventional strain measurements. These transient current signals thus provide a real-time probe of the micromechanics of asperity/surface interactions, with potentially submicrosecond time resolution. An area of potential importance of these studies is in systems where separated charges could make significant contributions to adhesion, e.g., moving interfaces in microelectromechanical systems devices which involve small mass/surface area ratios.

ACKNOWLEDGMENTS

The authors thank Mary Dawes for acquiring the SEM images. This work was supported by the National Science Foundation under Grant No. CMS-01-16196, an associated REU, and a subcontract with the University of Florida on a KDI-NSF Collaboration, Grant No. DMR-99-80015.

[1] K. C. Ludema, in *Friction, Lubrication, and Wear Technology,* edited by Peter J. Blau (American Society for Metals, Metals Park, OHI, 1992), Vol. 18, p. 236.
[2] K. A. Zimmerman, S. C. Langford, and J. T. Dickinson, J. Appl. Phys. **70**, 4808 (1991).
[3] J. T. Dickinson, L. C. Jensen, S. Lee, L. Scudiero, and S. C. Langford, J. Adhes. Sci. Technol. **8**, 1285 (1994).
[4] S. Lee, L. C. Jensen, S. C. Langford, and J. T. Dickinson, J. Adhes. Sci. Technol. **9**, 1 (1995).
[5] L. Scudiero, S. C. Langford, and J. T. Dickinson, in *Proceedings of the First International Congress on Adhesion Science and Technology,* edited by Jr. W. J. Van Ooij and H. R. Anderson (VSP, Zeist, The Netherlands, 1998), p. 597.
[6] L. Scudiero, S. C. Langford, and J. T. Dickinson, in *Proceedings of the First International Congress on Adhesion Science and Technology* (VSP, Zeist, The Netherlands, 1998), p. 585.
[7] J. T. Dickinson, S. C. Langford, S. Nakahara, L. Scudiero, M. W. Kim, and N.-S. Park, in *Fractography of Glasses and Ceramics III,* edited by J. R. Varner, V. D. Fréchette, and G. D. Quinn (American Ceramic Society, Westerville, Ohio, 1996), Vol. 64, p. 193.
[8] L.-H. Lee, in *Adhesive Bonding,* edited by L.-H. Lee (Plenum, New York, 1991), p. 1.
[9] M.-W. Kim, S. C. Langford, and J. T. Dickinson, Tribol. Lett. **1**, 147 (1995).
[10] J. T. Dickinson, L. Scudiero, K. Yasuda, M.-W. Kim, and S. C. Langford, Tribol. Lett. **3**, 53 (1997).
[11] J. T. Dickinson and E. E. Donaldson, J. Adhes. **24**, 199 (1987).
[12] Z.-Y. Ma, J.-W. Fan, and J. T. Dickinson, J. Adhes. **25**, 63 (1988).

[13] E. E. Donaldson and J. T. Dickinson, J. Adhes. **30**, 13 (1989).
[14] J. T. Dickinson, in *Non-Destructive Testing of Fibre-Reinforced Plastic Composites*, edited by J. Summerscales (Elsevier, London, 1990), p. 429.
[15] J. T. Dickinson, L. C. Jensen, and R. P. Dion, J. Appl. Phys. **73**, 3047 (1993).
[16] J. Lowell and A. C. Rose-Innes, Adv. Phys. **29**, 947 (1980).
[17] D. J. Montgomery, Solid State Phys. **9**, 139 (1959).
[18] M. Meunier and N. Quirke, J. Chem. Phys. **113**, 369 (2000).
[19] Jan J. Tuma, *Handbook of Physical Calculations*, 2nd ed. (McGraw–Hill, New York, 1983).
[20] M. R. Schroeder, *Fractals, Chaos, Power Laws* (W. H. Freeman, New York, 1991).
[21] F. C. Moon, *Chaotic and Fractal Dynamics* (Wiley, New York, 1992).
[22] J. E. Mark, A. Eisenberg, W. W. Graessely *et al.*, *Physical Properties of Polymers* (American Chemical Society, Washington, DC, 1984).
[23] J. V. Wasem, S. C. Langford, and J. T. Dickinson, (unpublished).
[24] B. B. Mandelbrot, *The Fractal Geometry of Nature* (Freeman, New York, 1983).
[25] L.-H. Lee, J. Electrost. **32**, 1 (1994).
[26] J. Lowell, J. Phys. D **17**, L233 (1977).
[27] J. Lowell, J. Phys. D **12**, 2217 (1979).
[28] D. K. Davies, Brit. J. Appl. Phys. Ser. 2 **2**, 1533 (1969).
[29] T. J. Fabish and C. B. Duke, J. Appl. Phys. **48**, 4256 (1977).
[30] A. R. Akande and J. Lowell, J. Phys. D **20**, 565 (1987).
[31] Y. Murata and I. Hiyoshi, J. Electrost. **46**, 143 (1999).
[32] W. J. Brennan, J. Lowell, M. C. O'Neill, and M. P. W. Wilson J. Phys. D **25 (10)**, 1513 (1992).
[33] T. J. Fabish, H. M. Saltsburg, and M. L. Hair, J. Appl. Phys. **47**, 940 (1976).
[34] W. Possart and A. Röder, Phys. Status Solidi A **84**, 319 (1984).
[35] W. Possart, Internat. J. Adhesion Adhesives **8**, 77 (1988).
[36] R. H. Partridge, J. Polym. Sci. A **3**, 2817 (1965).
[37] D. A. Hays, J. Chem. Phys. **61**, 1455 (1974).
[38] J. Lowell, J. Phys. D **10**, 65 (1977).
[39] A. Wåhlin and G. Bäckström, J. Appl. Phys. **45**, 2058 (1974).
[40] K. Li, B. Y. Ni, and J. C. M. Li, J. Mater. Res. **11**, 1574 (1996).
[41] C. Bauwens-Crowet, J. C. Bauwens, and G. Homès, J. Polym. Sci. Part A **A-2 7**, 735 (1969).
[42] N. W. J. Brooks, R. A. Duckett, and I. M. Ward, J. Polym. Sci., Part B: Polym. Phys. **36**, 2177 (1998).
[43] B. J. Briscoe, S. K. Biswas, S. K. Sinha, and S. S. Panesar Tribol. Int. **26**, 183 (1993).